

# **Substitution Effect on Phenalenyl Backbone in the Rate of Organozinc Catalyzed ROP of Cyclic Esters**

Tamal K. Sen, Arup Mukherjee, Arghya Modak, Swadhin K. Mandal,\* Debasis Koley.

*Department of Chemical Sciences, Indian Institute of Science Education and Research-Kolkata,  
Mohanpur -741252, India*

Email: swadhin.mandal@iiserkol.ac.in

### Packing diagram of complex 4, 5, 6:

The phenalenyl based organozinc complexes **4**, **5**, and **6** show a  $\pi$ -stacking on one over another in their crystal packing diagram. The interplaner distance between the  $\pi$ -stacked molecules of **4**, **5** and **6** are found 3.351 Å, 3.364 Å, and 3.770 Å respectively.

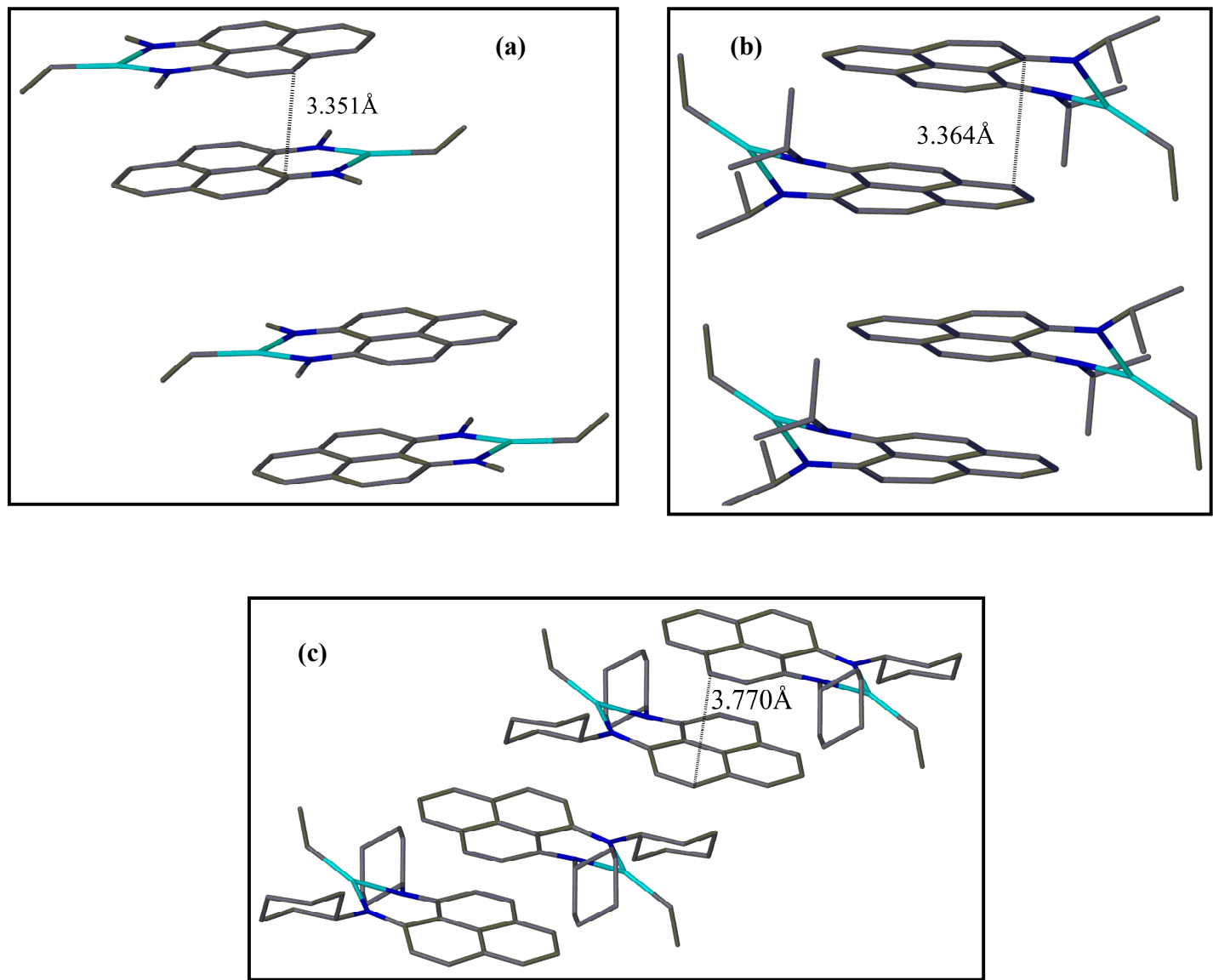
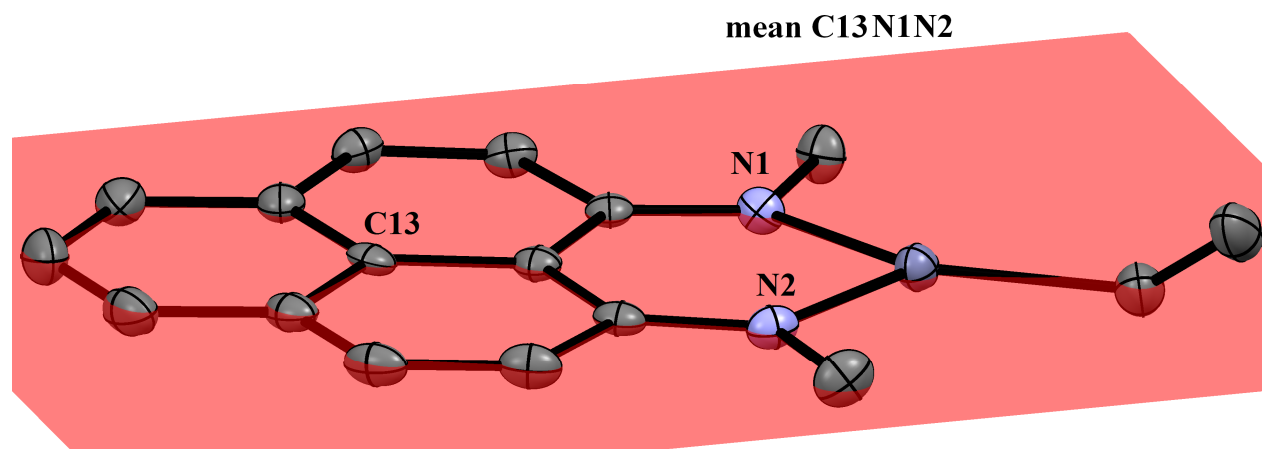


**Fig. S1** Packing diagram of phenalenyl zinc complexes (a) Packing diagram of complex **4**, (b) Packing diagram of complex **5**, and (c) Packing diagram of complex **6**.

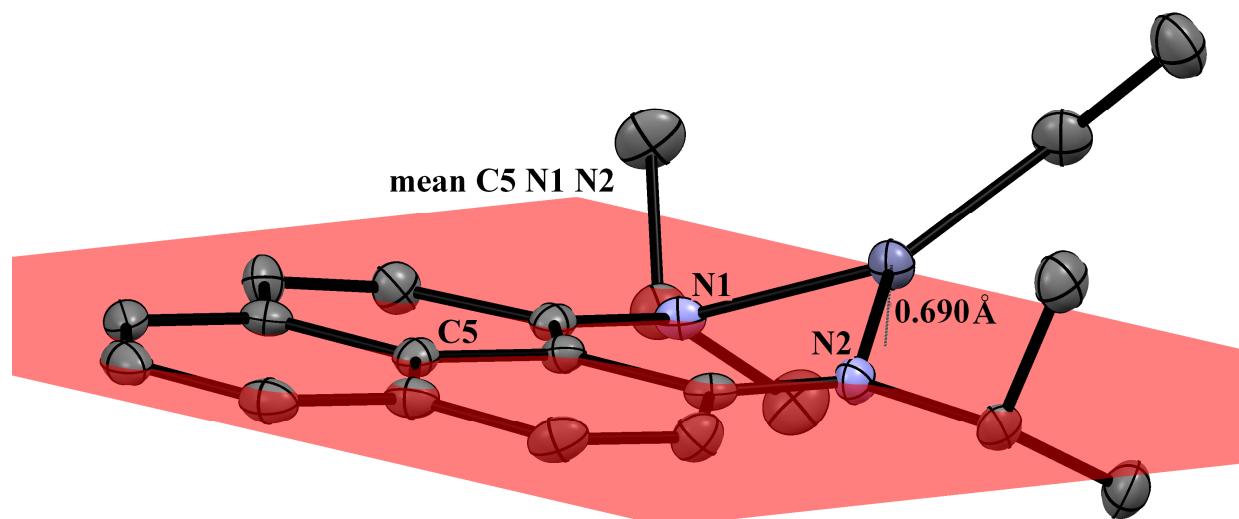
### Deviation of Zn centre from planarity

Substituted bulky alkyl group of N,N phenalenyl system interact with the zinc centre hence there is a deviation of zinc ion from the planarity. We determined the deviation from a reference plane defined by two coordinating nitrogen atoms and the central carbon atom of planer phenalenyl ligand (C13 in **4**, C5 in **5**, and C19 in **6**) from X-ray structural data.

(a)



(b)



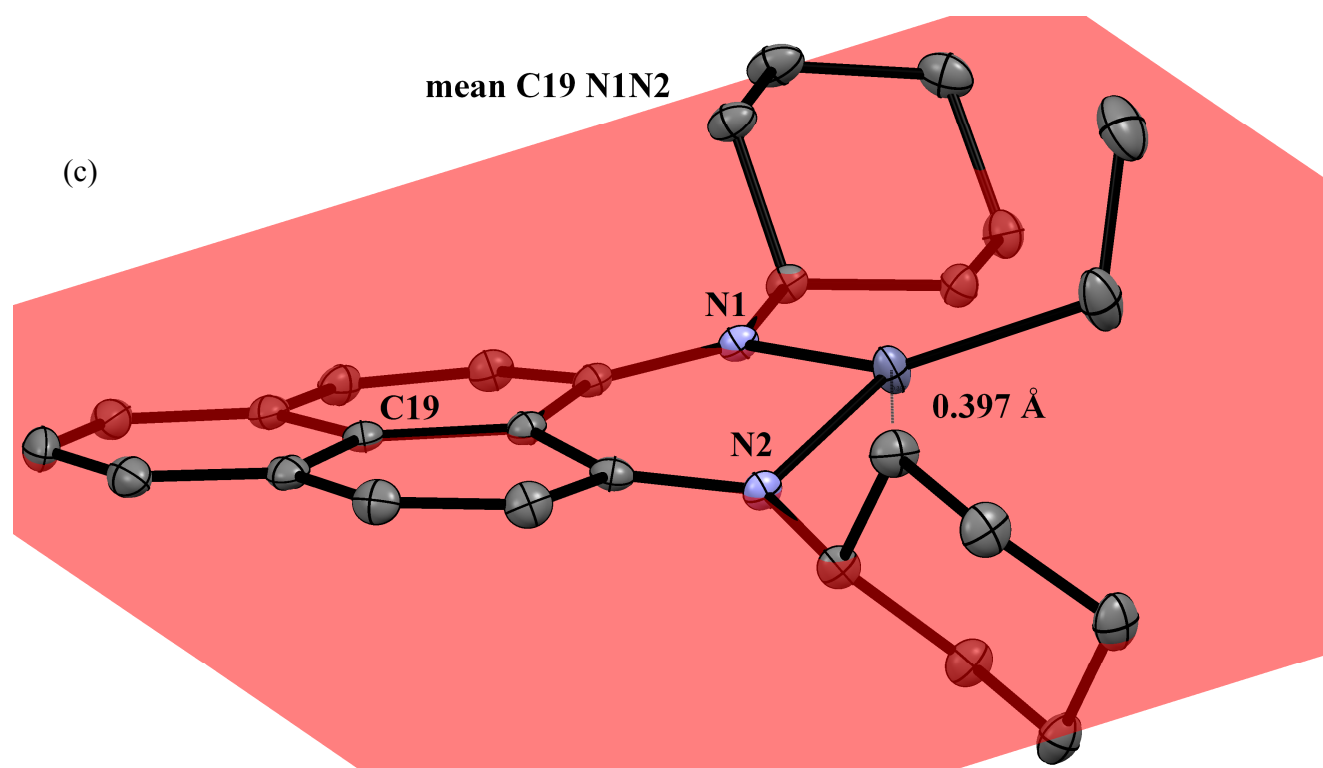


**Fig. S2** Deviation from planarity of zinc centre in the solid state structure of phenalenyl zinc complexes (a) 0 Å in **4**, (b) 0.397 Å in **5** and (c) 0.690 Å in **6**.

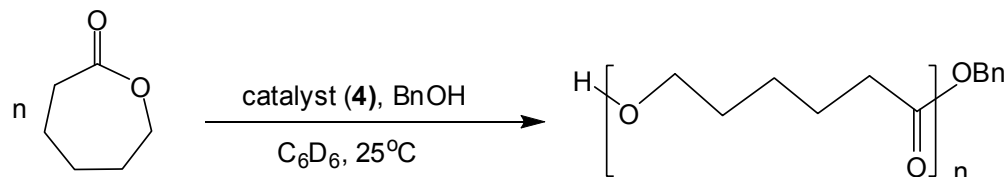
**Table S1. Crystal and Structure Refinement Parameters for Zinc Phenalenyl Complexes (1-6).**

Complex	1	2	3	4	5	6
Formula	C <sub>19</sub> H <sub>20</sub> O <sub>3</sub> Zn	C <sub>32</sub> H <sub>28</sub> N <sub>2</sub> O <sub>2</sub> Zn. C <sub>4</sub> H <sub>8</sub> O	C <sub>42</sub> H <sub>46</sub> N <sub>2</sub> O <sub>2</sub> Zn <sub>2</sub>	C <sub>17</sub> H <sub>18</sub> N <sub>2</sub> Zn	C <sub>21</sub> H <sub>29</sub> N <sub>2</sub> Zn	C <sub>27</sub> H <sub>34</sub> N <sub>2</sub> Zn
CCDC no.	873461	873462	873463	873464	873465	873466

Fw	361.73	610.05	741.59	315.73	374.83	451.96
cryst size/mm	0.14 x 0.19 x 0.20	0.15x 0.27 x 0.30	0.10 x 0.15 x 0.25	0.23 x 0.25 x 0.30	0.07x 0.12 x 0.25	0.10x 0.20x0.30
cryst syst	Triclinic	Monoclinic	Triclinic	Monoclinic	Triclinic	Monoclinic
space group	<i>P</i> ī	<i>C</i> 2	<i>P</i> ī	<i>P</i> 2 <sub>1</sub> /c	<i>P</i> ī	<i>P</i> 2 <sub>1</sub> /c
<i>a</i> /Å	8.8426(17)	15.731(2)	9.0529(16)	11.6112(5)	8.8105(8)	10.008(2)
<i>b</i> /Å	8.9066(17)	8.6745(12)	9.7356(17)	10.9964(5)	13.5563(9)	12.724(3)
<i>c</i> /Å	20.634(4)	11.5672(16)	10.5930(18)	11.2447(5)	15.6938(14)	17.615(4)
<i>a</i> /deg	90.296(4)	90	108.236(3)	90	74.278(2)	90
<i>β</i> /deg	91.322(3)	106.024(3)	102.958(3)	99.318(3)	83.9410(10)	105.050(4)
<i>γ</i> /deg	92.285(4)	90	95.965(3)	90	89.588(2)	90
<i>V</i> /Å <sup>3</sup>	1623.4(5)	1517.1(4)	848.7(3)	1416.79(11)	1793.8(3)	2166.2(8)
<i>D</i> <sub>calcd</sub> /g cm <sup>-3</sup>	1.480	1.336	1.451	1.480	1.377	1.386
<i>Z</i>	4	2	1	4	4	4
abs coeff/mm <sup>-1</sup>	1.525	0.844	1.454	1.724	1.373	1.151
θ range/deg	1.0 to 27.0	1.8 to 27.0	2.1to 27.0	1.8 to 27.0	1.4 to 27.0	2.0 to 27.0
reflns collected/ind ep reflns	26833/ 7059	6598/ 2836	13708/ 3719	26746/ 3096	11182/ 7531	44148/ 4729
max. and min.	0.808 and 0.744	0.881and 0.776	0.795 and 0.668	0.673 and 0.602	0.908 and 0.821	0.891 and 0.759
Transmn						
final <i>R</i> indices [ <i>I</i> > 2σ( <i>I</i> )]	R1= 0.0308, wR2= 0.0783	R1= 0.0253, wR2= 0.0575	R1= 0.0456, wR2=0.1246	R1= 0.0240, wR2=0.0971	R1=0.0363, wR2=0.0857	R1=0.0251, wR2=0.0651
<i>R</i> indices (all data)	R1= 0.0380,	R1= 0.0265,	R1= 0.0485	R1=0.0265	R1= 0.0525	R1=0.0313

	wR2= 0.0827	wR2= 0.0581	wR2=0.1275	wR2=0.1045	wR2= 0.1018	wR2=0.0694
largest diff peak and hole/e Å <sup>3</sup>	0.675 and -0.667	0.325 and -0.233	3.550 and -0.423	0.608 and -0.338	0.535 and -0.343	0.427 and -0.437

### NMR monitoring polymerization of $\epsilon$ -Caprolactone in $C_6D_6$ with complex 4 as catalyst.



The progress of the polymerization reaction of  $\epsilon$ -caprolactone in  $C_6D_6$  using catalyst 4 was monitored by in situ  $^1H$  NMR spectroscopic studies. Figure S3 reveals a clean conversion of the substrate to the polymerization product with gradual progress of time.

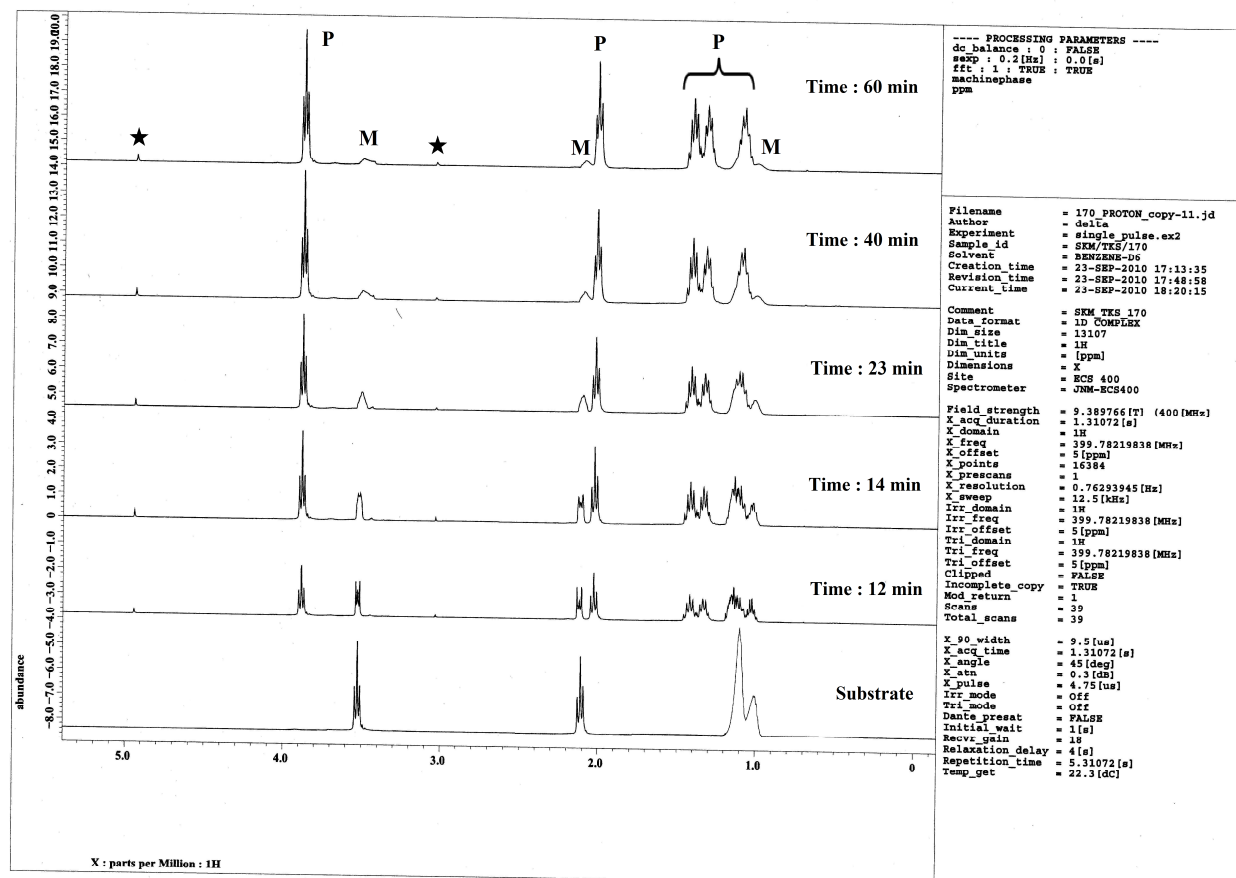


**Fig. S3** Stack plot of  $^1H$  NMR spectra in  $C_6D_6$  for the polymerization of  $\epsilon$ -caprolactone with 4 recorded at different time intervals at 25 °C. P, M, ★ are the peak due to polymer, monomer and end group benzyl alcohol respectively.

**Kinetics experiments of  $\varepsilon$ -CL polymerization using organozinc complex 4, 5 and 6.**

The molecular weights of the ring-opened polymers can be controlled as a function of the monomerto-initiator ratio (M/I) with consistently narrow polydispersities (PDIs). The plot of molecular weight [ $M_n$ (GPC)] versus percent of conversion is presented shows the gradual increase of molecular weight in a linear fashion with progress of the polymerization . This result indicates the controlled nature of polymerization. Also the PDI values remain almost constant during the course of polymerization further supporting the controlled nature of polymerization process (Fig. S1). The polymerization was performed inside a nitrogen filled glovebox using toluene as solvent. In a single necked tube fitted with standard ground joint, a toluene solution of catalyst (0.033 mmol, 1.0 mL toluene) and BnOH (0.033 mmol) were loaded inside the N<sub>2</sub> filled glovebox at room temperature. The solution was stirred for 5 min, and  $\varepsilon$ -caprolactone (3.33 mmol) along with 1.5 mL toluene solution and the tube was closed with a glass stopper. The reaction mixture was stirred at 25°C. Kinetic experiments were performed by taking a small amount of aliquots (150 $\mu$ L) from the reaction mixture after a certain time interval and quenched by the addition of water (100  $\mu$ L). Subsequently, the reaction mixture was dried and checked by <sup>1</sup>H NMR spectroscopy and GPC analysis. The conversion as well as the  $M_n$ (GPC) at different time interval were determined from the <sup>1</sup>H NMR spectroscopy . The relative molecular weight with respect to polystyrene standard and the poly dispersity index (PDI) values were determined from the GPC measurements.

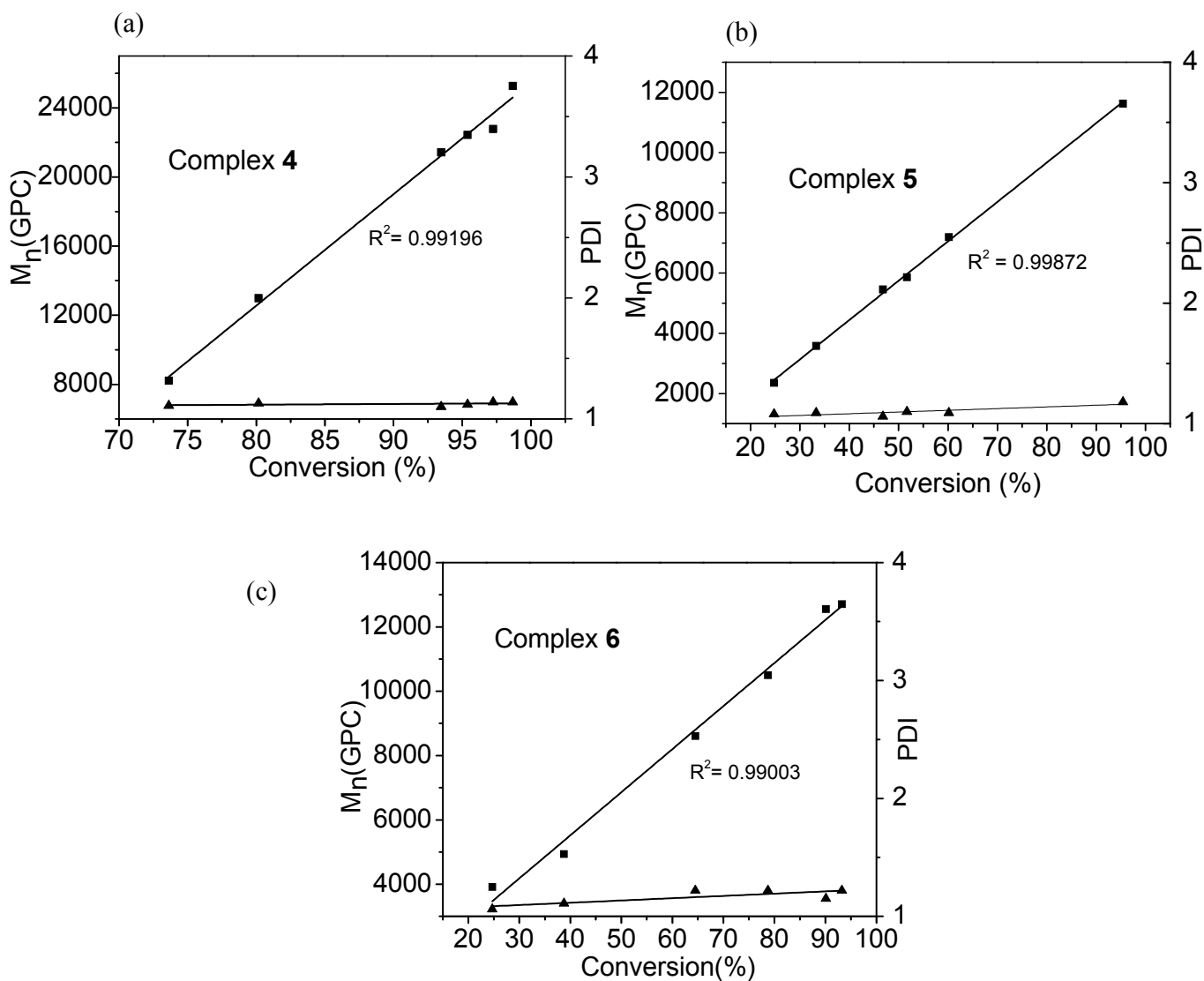


**Fig. S4** Polymerization of  $\epsilon$ -caprolactone using phenalenyl based ethylzinc complexes (**4–6**) as catalysts; polymerization carried out in 2.5 mL of toluene at 25°C the ratio of  $[\epsilon\text{-CL}]_0/[\text{catalyst}]/[\text{BnOH}] = 100:1:1$  used. Plots of  $M_n$  and PDI (determined by GPC) vs. conversion of  $\epsilon$ -caprolactone using catalysts (a) **4**, (b) **5**, and (c) **6**. The ratio of  $[\epsilon\text{-CL}]_0/[\text{catalyst}]/[\text{BnOH}] = 100:1:1$  used. Square signs (■) represent  $M_n$  values and triangle signs (▲) represent PDI values.

### Kinetics experiments of *rac*-LA polymerization using organozinc complex 4, 5 and 6.

The molecular weights of the ring-opened polymers can be controlled as a function of the monomerto-initiator ratio (M/I) with consistently narrow polydispersities (PDIs). The plot of molecular weight [ $M_n$ (GPC)] versus percent of conversion is presented shows the gradual increase of molecular weight in a linear fashion with progress of the polymerization . This result indicates the controlled nature of polymerization. Also the PDI values remain almost constant during the course of polymerization further supporting the controlled nature of polymerization process (Fig. S1). The polymerization was performed inside a nitrogen filled glovebox using toluene as solvent. In a single necked tube fitted with standard ground joint, a toluene solution of catalyst (0.026 mmol, in 1.0 mL toluene) and BnOH (0.026 mmol) were loaded inside the glovebox at room temperature. The solution was stirred for 5 min, and *rac*-lactide (2.60 mmol) along with 4.0 mL toluene was added to the solution and the tube was closed with a glass stopper. The reaction mixture was subsequently stirred at required temperature. Kinetic experiments were performed by taking a small amount of aliquots (150 $\mu$ L) from the reaction mixture after a certain time interval and quenched by the addition of water (100  $\mu$ L). Subsequently, the reaction mixture was dried and checked by  $^1$ H NMR spectroscopy and GPC analysis. The conversion as well as the  $M_n$ (GPC) at different time interval were determined from the  $^1$ H NMR spectroscopy . The relative molecular weight with respect to polystyrene standard and the poly dispersity index (PDI) values were determined from the GPC measurements.

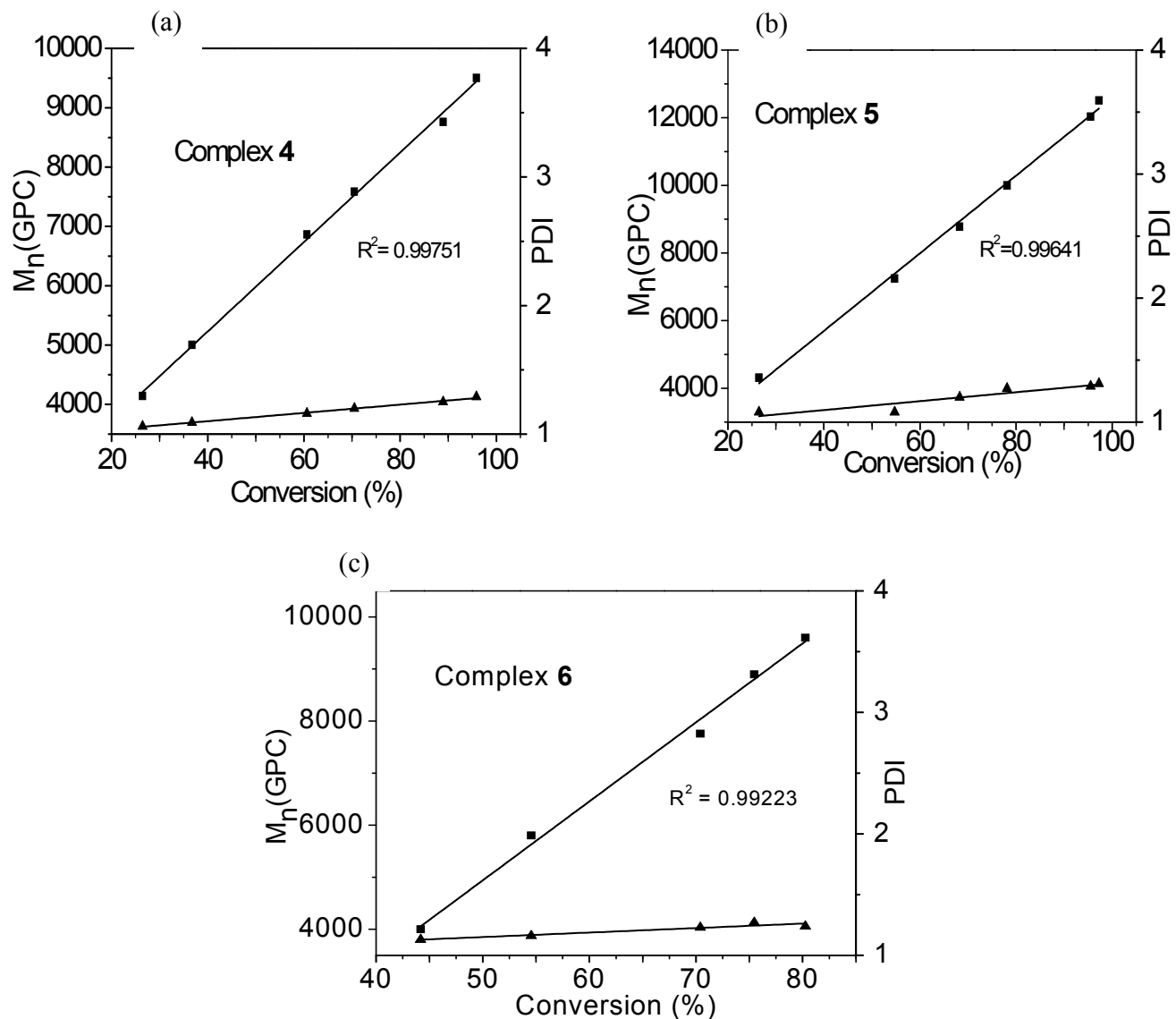


**Fig. S5** Polymerization of *rac*-LA using phenalenyl based organozinc complexes (**4-6**) using  $[rac\text{-LA}]_0/[catalyst]/[BnOH] = 100:1:1$  ratio in 5 mL toluene at 50 °C. Plots of Mn and PDI (determined by GPC) vs. conversion of *rac*-LA using catalysts (a) **4**, (b) **5**, and (c) **6**. Square signs (■) represent Mn values and triangle signs (▲) represent PDI values.

### Homonuclear decoupling $^1\text{H}$ NMR spectra of poly(rac)lactide

We determined the microstructure of the poly(*rac*-LA) by using homonuclear decoupled  $^1\text{H}$  NMR spectroscopy which shows the homonuclear decoupled  $^1\text{H}$  NMR spectra in the methane range ( $\sim\delta 5.2$  ppm) of poly(*rac*-LA). The peaks were assigned to the appropriate tetrads as reported in literature.<sup>1</sup> The homonuclear decoupled  $^1\text{H}$  NMR spectra indicate the formation of heterotactic polylactide with the present zinc catalysts 4-6.

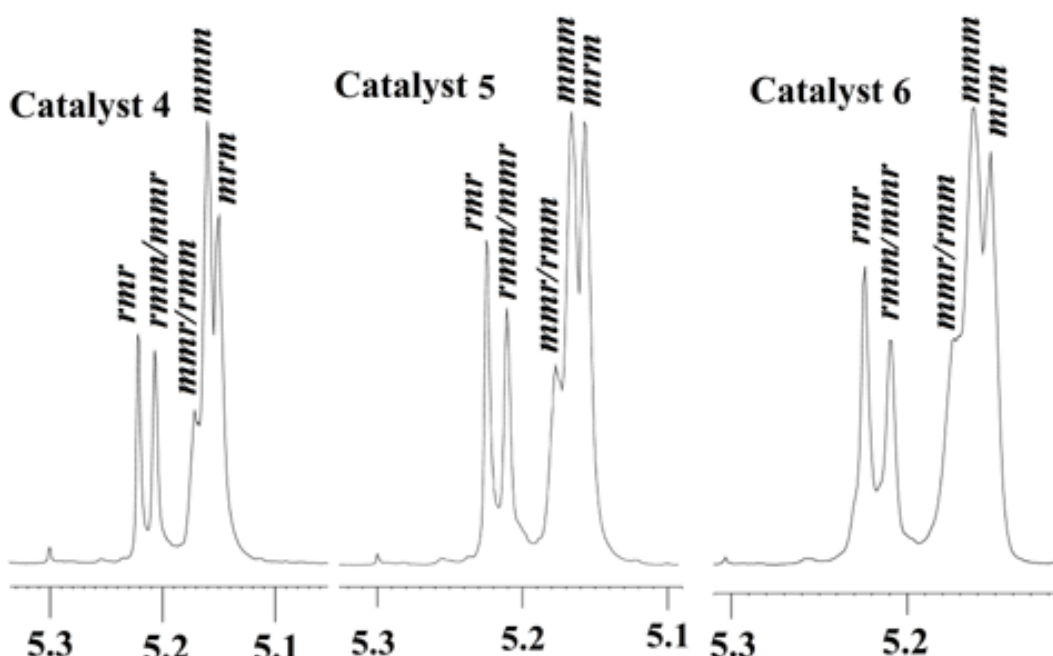


**Fig. S6** Homonuclear decoupled  $^1\text{H}$  NMR spectra ( $\text{CDCl}_3$ , 25 °C) of the methine range of poly(*rac*)lactide obtained from *rac*-LA using catalysts 4, 5, and 6.

## NMR spectra of the complexes

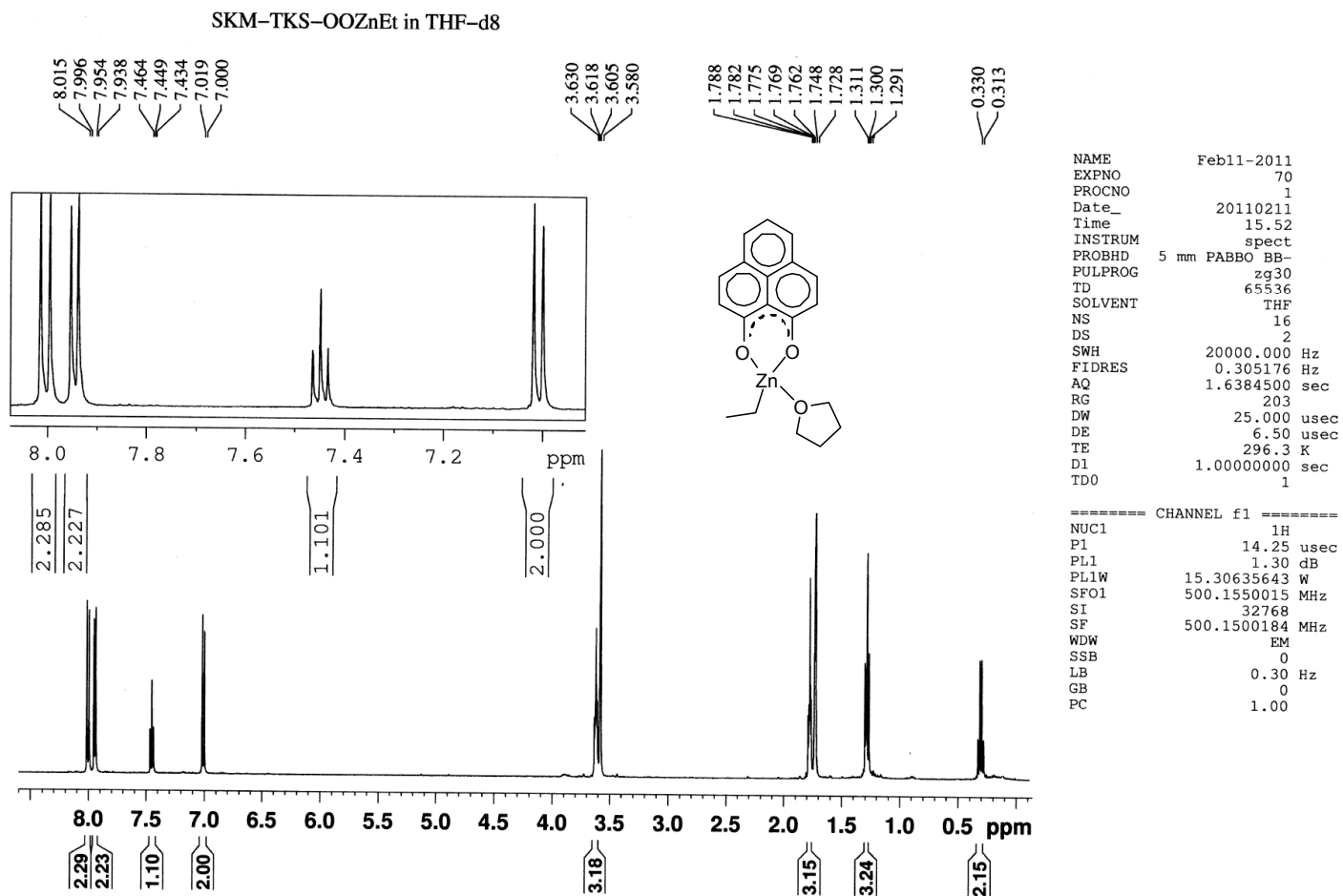


Fig. S7 <sup>1</sup>H NMR of compound 1 recorded in THF-d<sub>8</sub>.

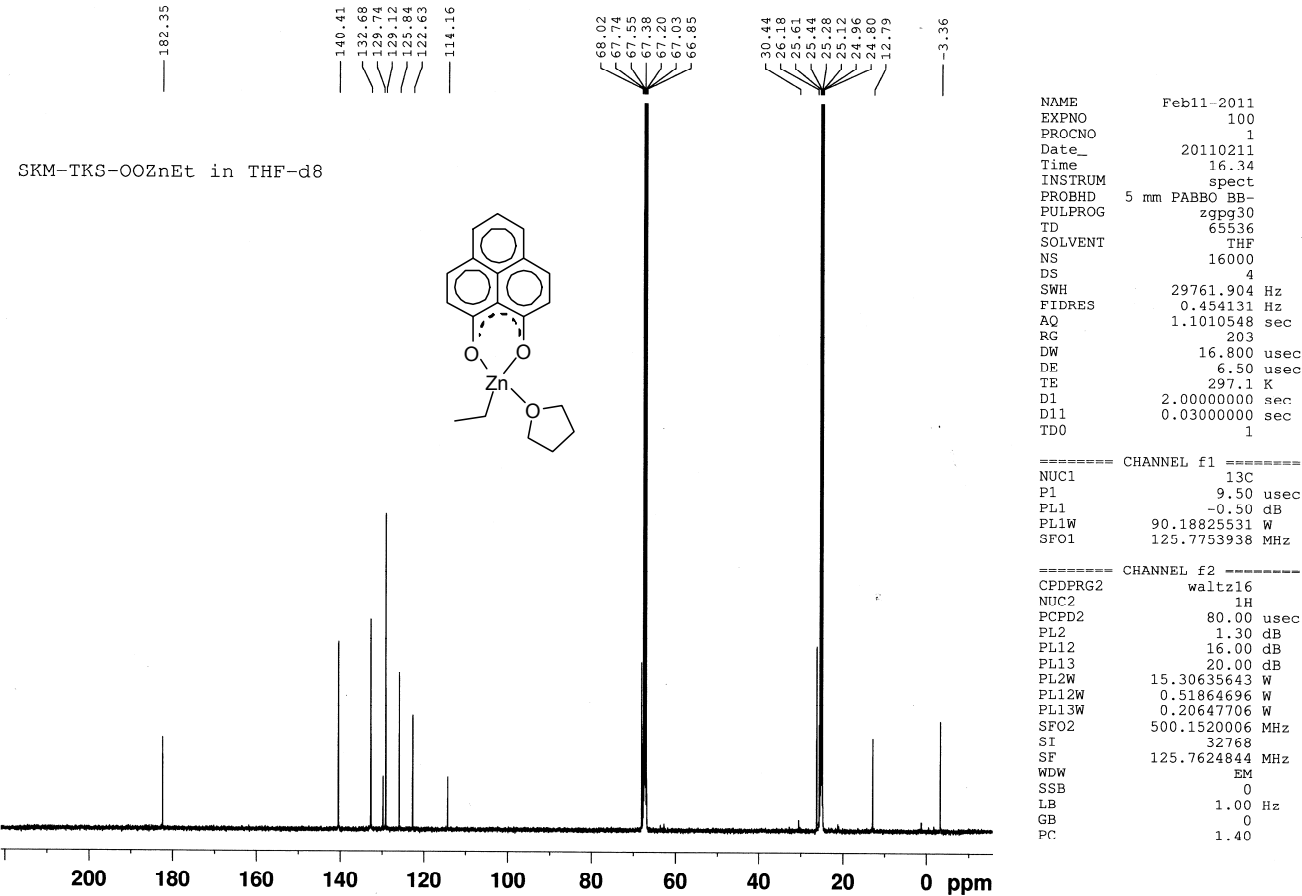
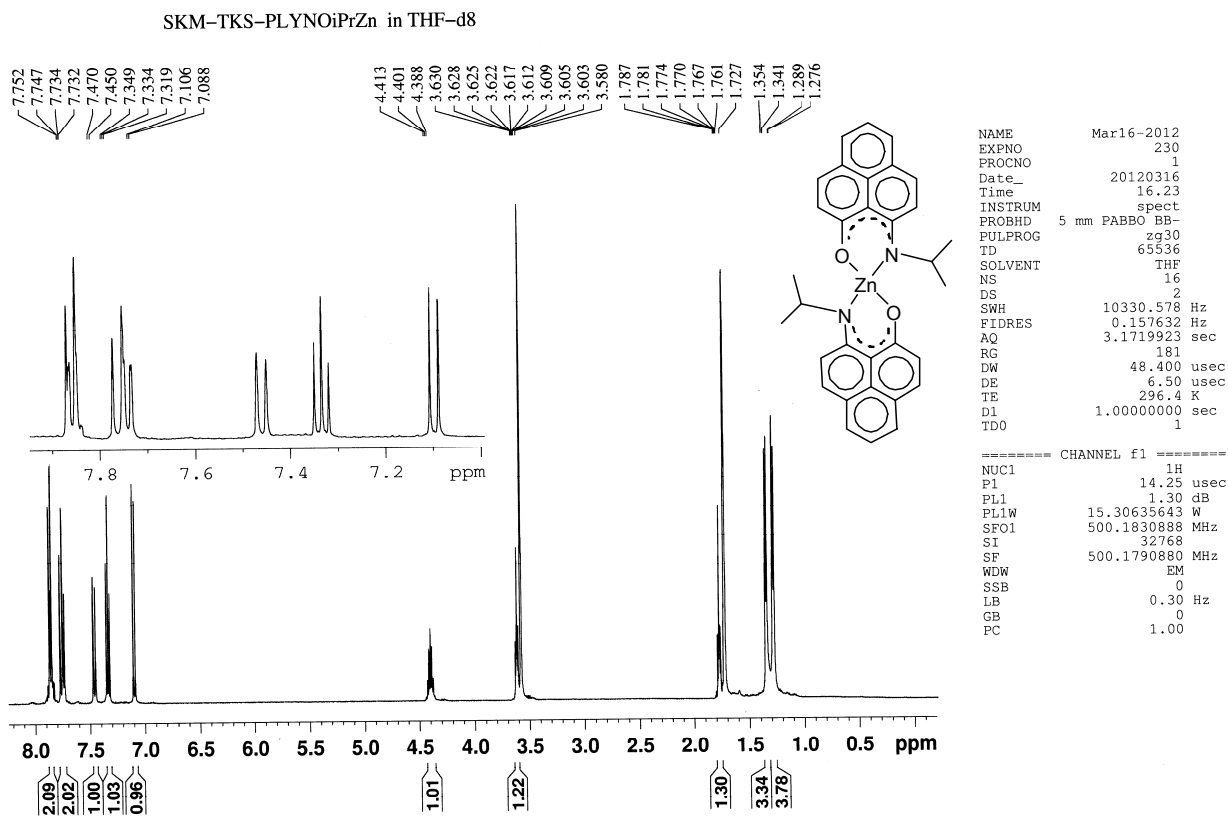
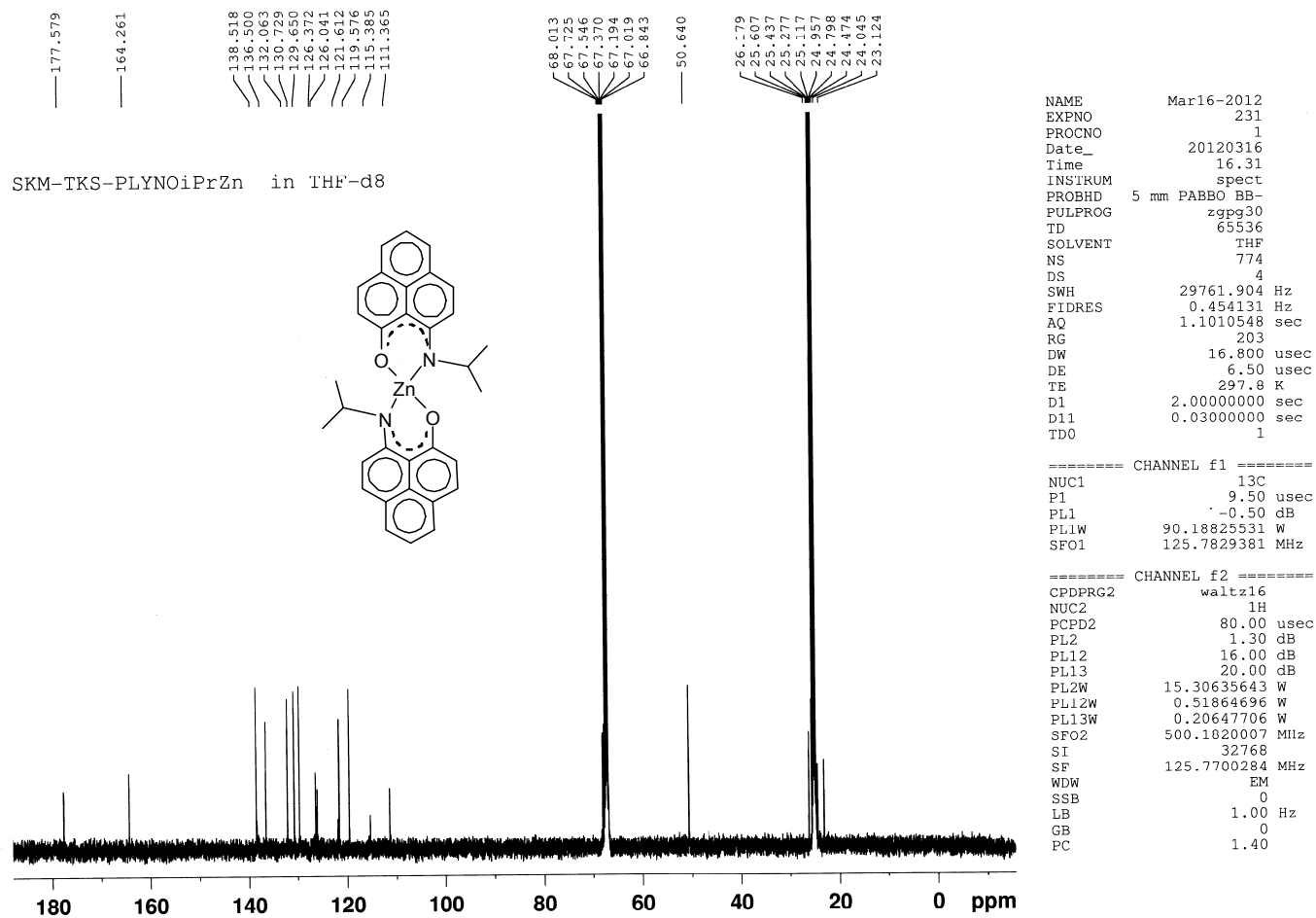


Fig. S8  $^{13}\text{C}$  NMR of compound **1** recorded in  $\text{THF}-\text{d}_8$ .



**Fig. S9** <sup>1</sup>H NMR of compound 2 recorded in THF-d<sub>8</sub>.



**Fig. S10** <sup>13</sup>C NMR of compound 2 recorded in THF-d<sub>8</sub>.

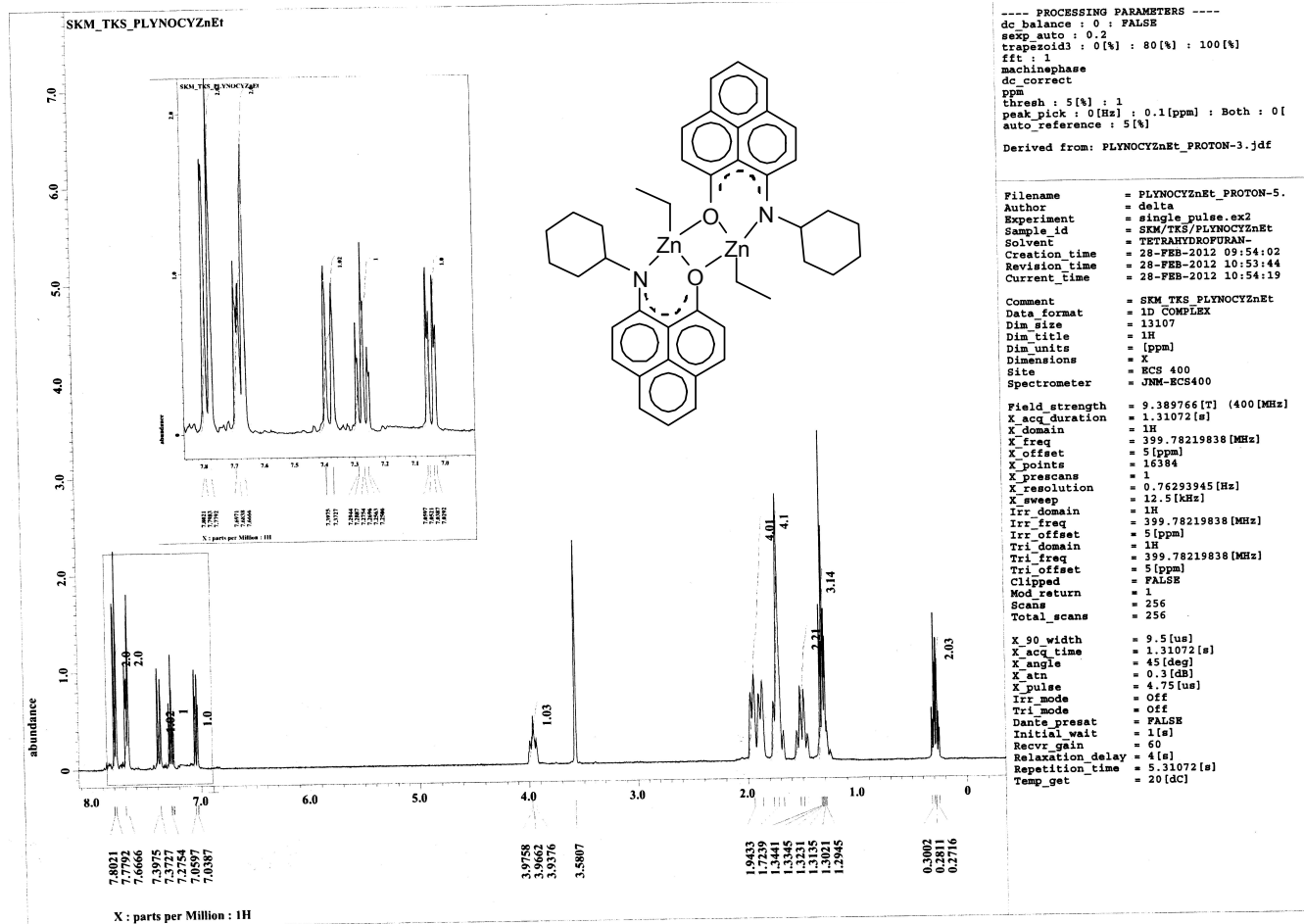
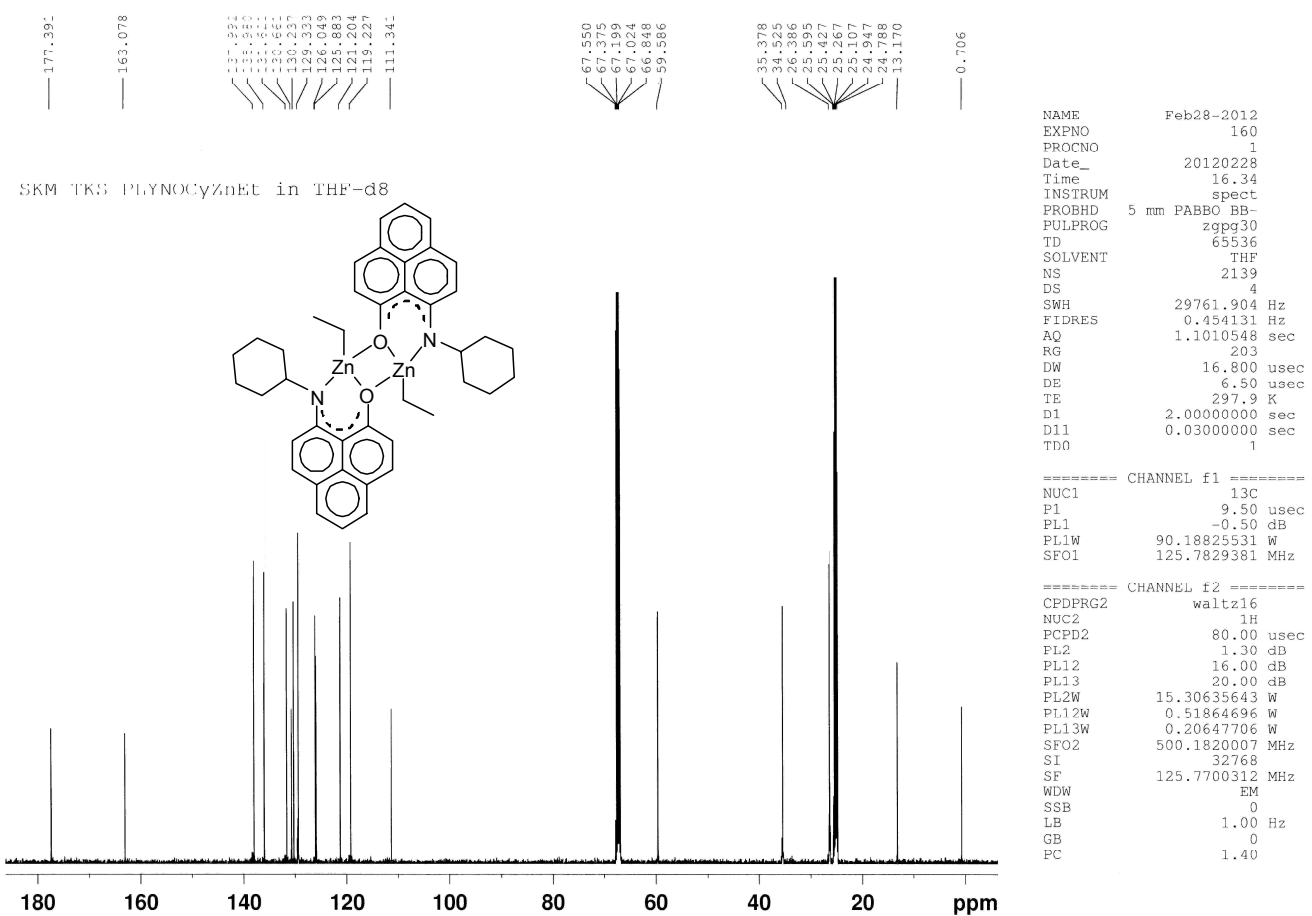
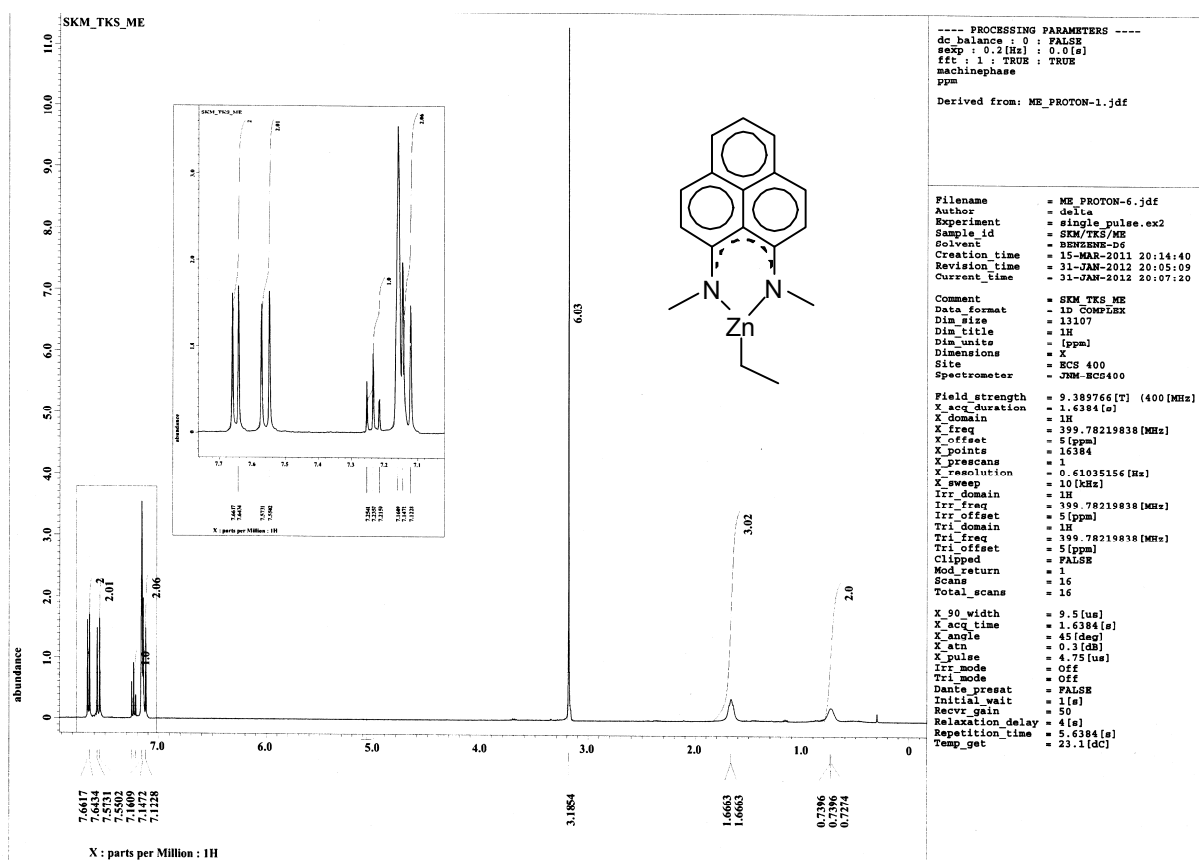


Fig. S11 <sup>1</sup>H NMR of compound 3 recorded in THF-d<sub>8</sub>.



**Fig. S12** <sup>13</sup>C NMR of compound 3 recorded in THF-d<sub>8</sub>.



**Fig. S13**  $^1\text{H}$  NMR of compound 4 recorded in  $\text{C}_6\text{D}_6$ .

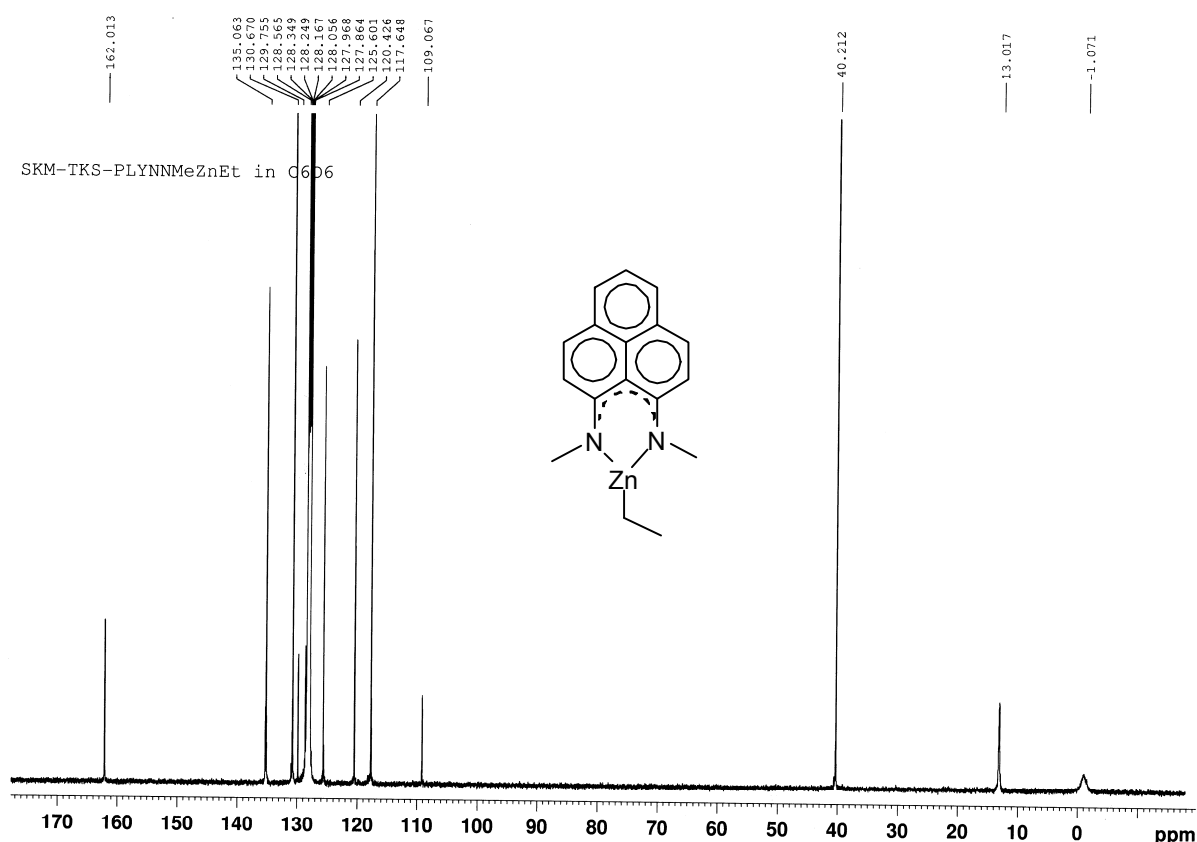


**Fig. S14** <sup>13</sup>C NMR of compound 4 recorded in C<sub>6</sub>D<sub>6</sub>.

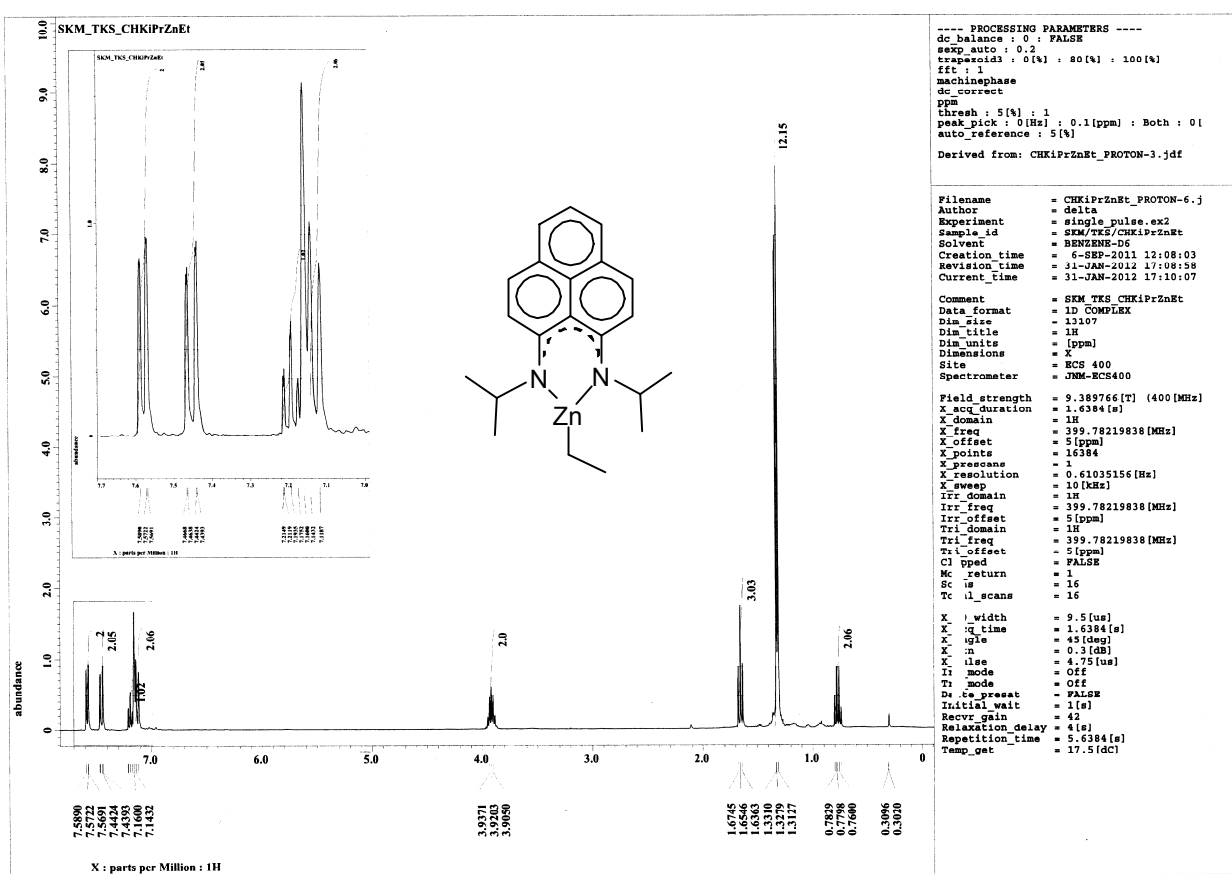


**Fig. S15**  $^1\text{H}$  NMR of compound **5** recorded in  $\text{C}_6\text{D}_6$ .

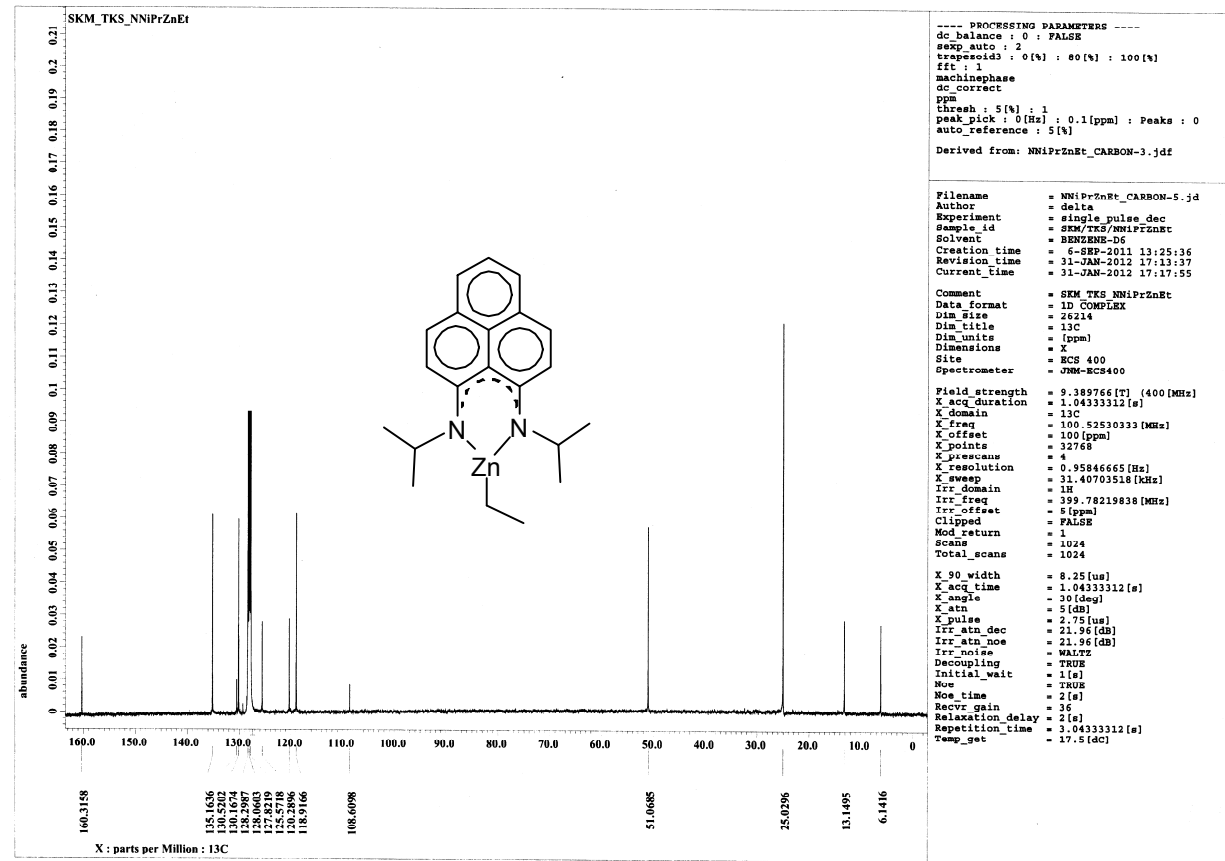


Fig. S16  $^{13}\text{C}$  NMR of compound 5 recorded in  $\text{C}_6\text{D}_6$ .

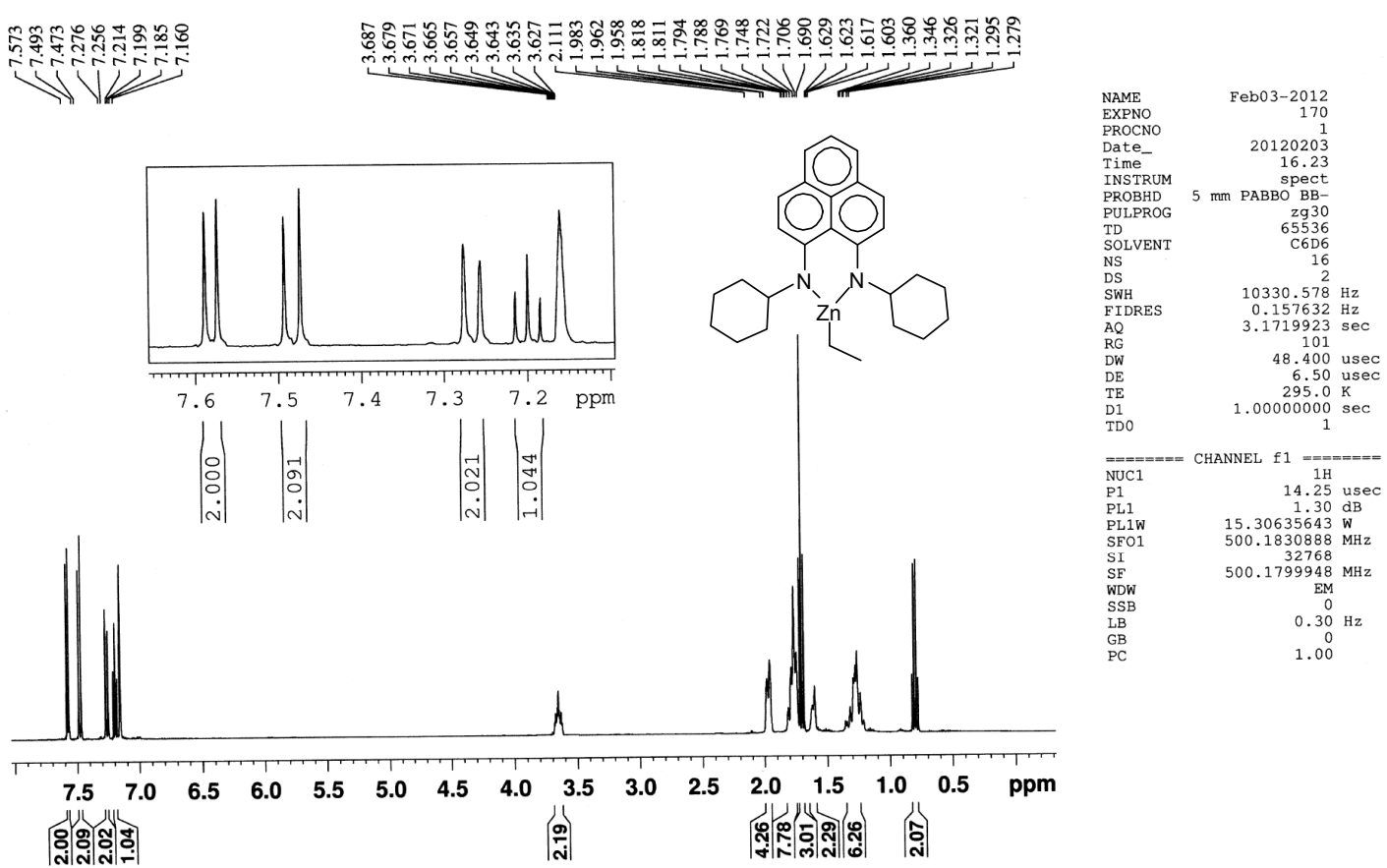
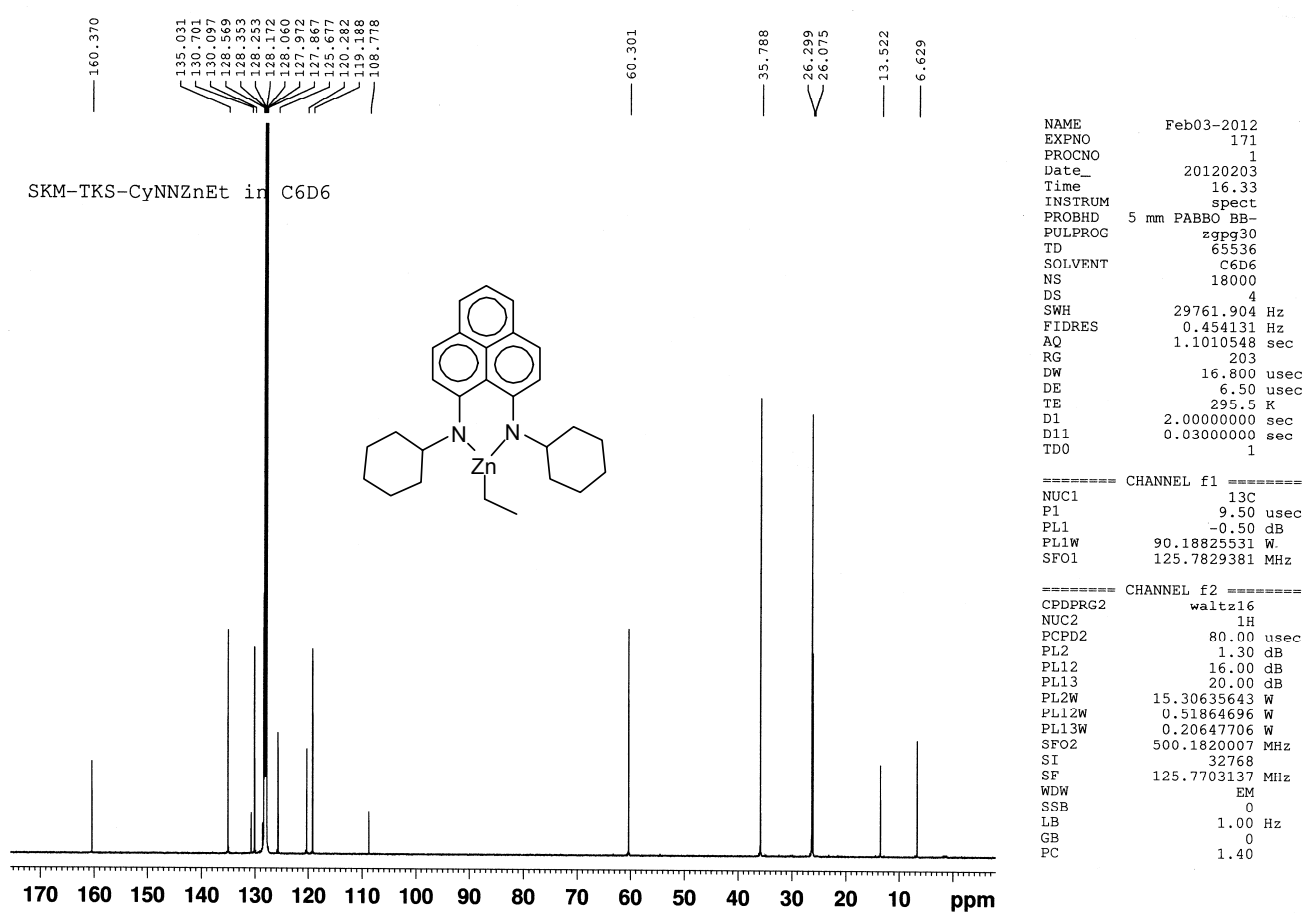


Fig. S17 <sup>1</sup>H NMR of compound 6 recorded in C<sub>6</sub>D<sub>6</sub>.



**Fig. S18** <sup>13</sup>C NMR of compound 6 recorded in C<sub>6</sub>D<sub>6</sub>.

### LUMO diagram of **4**, **5**, **6**.

DFT level calculations were performed on organozinc complexes **4**, **5** and **6**. The LUMOs of **4**, **5** and **6** are presented in Fig. S19. It is shown that the LUMO predominantly resides over the phenalenyl part of the molecule.

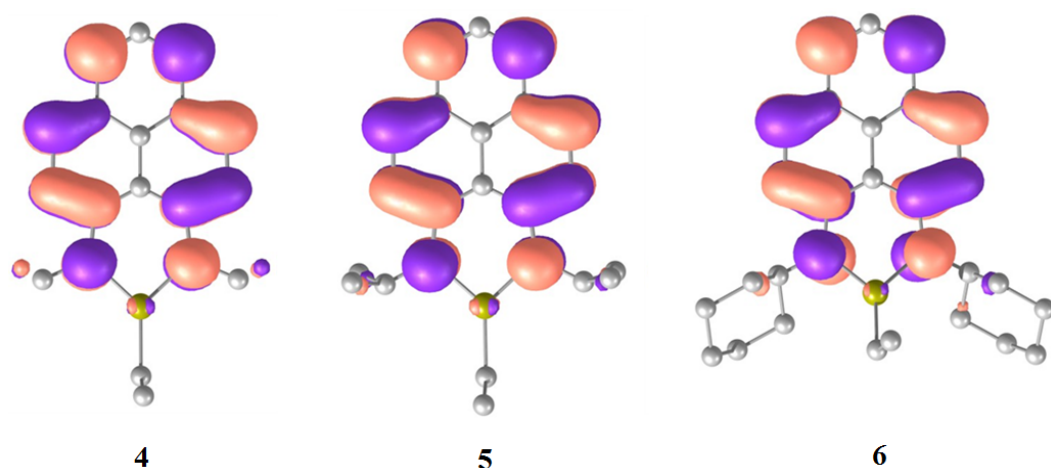


**Fig. S19** Computer generated LUMO of organozinc complexes **4**, **5**, and **6**.

## Atomic Co-ordinates of the Optimized Structures.

### Complex 4

Zn	-2.49933	0.00217	-0.19044
C	0.86253	0.00017	-0.04477
C	0.17930	-1.30123	-0.08466
C	0.18080	1.30238	-0.08393
C	2.30998	-0.00069	0.03417
C	1.00232	-2.49941	-0.04359
H	0.50349	-3.47529	-0.07246
C	3.07415	-1.22540	0.07503
C	2.36860	-2.46800	0.03349
H	2.94307	-3.40878	0.06468
C	3.07561	1.22311	0.07486
C	1.00529	2.49958	-0.04352
H	0.50763	3.47605	-0.07264
C	2.37155	2.46655	0.03308
H	2.94717	3.40665	0.06371
C	-1.73533	-2.79055	-0.20421
H	-1.38685	-3.37435	-1.08687
H	-2.83699	-2.70387	-0.27722
H	-1.50670	-3.38700	0.70890
C	4.48707	-1.20638	0.15340
H	5.02073	-2.17062	0.18246
C	-1.73221	2.79406	-0.19975
H	-1.50067	3.38959	0.71321
H	-2.83414	2.70879	-0.27021
H	-1.38512	3.37806	-1.08285
C	4.48851	1.20242	0.15316
H	5.02333	2.16602	0.18199
C	-4.46800	0.00291	-0.23794
C	5.20133	-0.00241	0.19304
H	6.30043	-0.00306	0.25359
C	-5.15957	-0.00842	1.14034
H	-4.88524	-0.90357	1.73962
H	-6.27101	-0.00788	1.05889
H	-4.88540	0.87701	1.75395
N	-1.16061	-1.44219	-0.15698
N	-1.15903	1.44496	-0.15476
H	-4.80395	0.89137	-0.81892
H	-4.80397	-0.87574	-0.83366

## Complex 5

Zn	2.20242	0.00271	0.15537
C	-1.13719	-0.00059	0.00943
C	-0.45510	-1.31072	0.04260
C	-0.45723	1.31083	0.03496
C	-2.59121	-0.00197	-0.05145
C	-1.29492	-2.49878	0.01727
H	-0.80397	-3.47440	0.04392
C	-3.36194	-1.22277	-0.07456
C	-2.65995	-2.46601	-0.03747
H	-3.23554	-3.40639	-0.05359
C	-3.36357	1.21735	-0.09155
C	-1.29838	2.49721	-0.01344
H	-0.80858	3.47368	-0.00278
C	-2.66314	2.46189	-0.07292
H	-3.23971	3.40117	-0.10740
C	1.57549	-2.78388	0.12555
H	2.64838	-2.49514	0.15887
C	-4.77580	-1.20637	-0.13157
H	-5.30678	-2.17242	-0.14594
C	1.56881	2.78842	0.14608
H	2.64136	2.50210	0.20307
C	-4.77736	1.19829	-0.14912
H	-5.30957	2.16333	-0.17816
C	4.17480	0.00327	0.24242
C	-5.49289	-0.00471	-0.16890
H	-6.59278	-0.00576	-0.21283
C	4.89554	-0.00692	-1.12071
H	4.63366	-0.90159	-1.72639
H	6.00521	-0.00632	-1.01713
H	4.63381	0.87884	-1.73934
N	0.88503	-1.45610	0.09410
N	0.88203	1.45905	0.10091
H	4.49993	0.89076	0.83134
H	4.49945	-0.87547	0.84460
C	1.46559	3.61779	-1.15303
H	2.22349	4.42887	-1.13258
H	1.67857	2.97866	-2.03423
H	0.47786	4.09282	-1.31488
C	1.31943	3.59716	1.43740
H	2.05153	4.42969	1.49904
H	0.30642	4.04006	1.50729
H	1.46514	2.95234	2.32806
C	1.44452	-3.61393	-1.17037
H	1.64246	-2.97614	-2.05602
H	2.19987	-4.42764	-1.16399
H	0.45200	-4.08518	-1.31235
C	1.35705	-3.59234	1.42282
H	2.09531	-4.42032	1.47094
H	1.51674	-2.94528	2.30948
H	0.34851	-4.04164	1.51407

## Complex 6

Zn	-1.42932	0.07424	0.42409
N	-0.13497	1.43045	-0.26074
N	-0.27146	-1.41588	-0.21300
C	1.20181	1.23900	-0.23070
C	1.82461	-0.09000	-0.10841
C	1.07642	-1.35620	-0.16183
C	-0.96359	-2.68053	-0.52267
C	-2.17054	-2.39665	-1.44500
C	-2.94397	-3.68134	-1.78925
C	-3.39356	-4.42611	-0.52043
C	-2.20144	-4.71612	0.40754
C	-1.41911	-3.43424	0.74856
C	1.84634	-2.59125	-0.13885
C	3.20777	-2.62419	-0.00175
C	3.97185	-1.41754	0.06927
C	5.38033	-1.46390	0.19815
C	6.15073	-0.29445	0.22994
C	5.50080	0.94079	0.11304
C	4.09409	1.02541	-0.01448
C	3.45311	2.29354	-0.17156
C	2.09358	2.38822	-0.29835
C	3.26888	-0.15905	-0.01202
C	-0.69791	2.76555	-0.53894
C	-0.93248	3.56631	0.76353
C	-1.56217	4.94348	0.48992
C	-2.86261	4.81878	-0.32148
C	-2.63495	4.02592	-1.62068
C	-2.01057	2.64519	-1.34427
C	-3.11867	0.19343	1.44804
C	-2.99409	-0.14084	2.94778
H	7.24574	-0.34567	0.33091
H	5.86588	-2.45141	0.26608
H	3.73254	-3.59190	0.06440
H	1.30539	-3.54488	-0.16439
H	4.07225	3.20611	-0.18246
H	1.65495	3.38801	-0.39705
H	-0.00189	3.34706	-1.18520
H	-0.28895	-3.35177	-1.10109
H	-0.53695	-3.66765	1.38291
H	-2.06009	-2.74878	1.34819
H	-1.81365	-1.88749	-2.36551
H	-2.85449	-1.68225	-0.93000
H	-2.29269	-4.35116	-2.39752
H	-1.95991	4.60693	-2.29126
H	-3.58956	3.90395	-2.17642
H	-3.63054	4.29781	0.29547
H	-1.80923	2.10295	-2.29299
H	-2.73428	2.02390	-0.76844
H	-1.60217	2.96668	1.42077
H	6.08211	1.87761	0.11096

H	-3.52736	1.22218	1.33129
H	-3.87293	-0.47596	0.97571
H	-2.27840	0.53206	3.46794
H	-2.63212	-1.17804	3.11927
H	-3.96574	-0.05069	3.48570
H	-1.51856	-5.44238	-0.09149
H	-2.54524	-5.20974	1.34215
H	-3.91443	-5.37086	-0.78800
H	-4.13825	-3.80211	0.02533
H	0.02641	3.67411	1.31458
H	-3.81856	-3.43753	-2.43010
H	-0.83736	5.57396	-0.07587
H	-3.27649	5.82481	-0.54978
H	-1.74887	5.47379	1.44871

### Full reference for Gaussian 03 Ref 34:

Gaussian 03, Revision B.03, M. J. Frisch, G. W. Trucks, H. B. Schlegel, G. E. Scuseria, M. A. Robb, J. R. Cheeseman, Jr., J. A. Montgomery, T. Vreven, K. N. Kudin, J. C. Burant, J. M. Millam, S. S. Iyengar, J. Tomasi, V. Barone, B. Mennucci, M. Cossi, G. Scalmani, N. Rega, G. A. Petersson, H. Nakatsuji, M. Hada, M. Ehara, K. Toyota, R. Fukuda, J. Hasegawa, M. Ishida, T. Nakajima, Y. Honda, O. Kitao, H. Nakai, M. Klene, X. Li, J. E. Knox, H. P. Hratchian, J. B. Cross, V. Bakken, C. Adamo, J. Jaramillo, R. Gomperts, R. E. Stratmann, O. Yazyev, A. J. Austin, R. Cammi, C. Pomelli, J. W. Ochterski, P. Y. Ayala, K. Morokuma, G. A. Voth, P. Salvador, J. J. Dannenberg, V. G. Zakrzewski, S. Dapprich, A. D. Daniels, M. C. Strain, O. Farkas, D. K. Malick, A. D. Rabuck, K. Raghavachari, J. B. Foresman, J. V. Ortiz, Q. Cui, A. G. Baboul, S. Clifford, J. Cioslowski, B. B. Stefanov, G. Liu, A. Liashenko, P. Piskorz, I. Komaromi, R. L. Martin, D. J. Fox, T. Keith, M. A. Al-Laham, C. Y. Peng, A. Nanayakkara, M. Challacombe, P. M. W. Gill, B. Johnson, W. Chen, M. W. Wong, C. Gonzalez and J. A. Pople, Gaussian, Inc., Wallingford CT, 2004.

### Reference:

- (1) (a) A. Pietrangelo, S. C. Knight, A. K. Gupta, L. J. Yao, M. A. Hillmyer and W. B. Tolman, *J. Am. Chem. Soc.* 2010, **132**, 11649–11657. (b) F. Drouin, P. O. Oguadinma, T. J. J. Whitehorne, R. E. Prud'homme and F. Schaper, *Organometallics* 2010, **29**, 2139–2147.